The contact mechanics challenge: Problem definition

Martin H. Müser[1, 2] and Wolf B. Dapp[1]

[1] *John von Neumann Institut für Computing and Jülich Supercomputing Centre,*
Institute for Advanced Simulation, FZ Jülich, 52425 Jülich, Germany
[2] *Department of Materials Science and Engineering,*
Saarland University, 66123 Saarbrücken, Germany
(Dated: April 4, 2016)

We present a contact mechanics problem, which we consider to be representative for contacts between nominally flat surfaces. The main ingredients of the mathematically fully defined contact problem are: Self-affine roughness, linear elasticity, the small-slope approximation, and short-range adhesion between the frictionless surfaces. Surface energies, elastic contact modulus and computer-generated surface topographies are provided at www.lms.uni-saarland.de/contact-mechanics-challenge. To minimize the undesirable but frequent problem of unit conversion errors, we provide some benchmark results, such as the relative contact area as a function of load $a_{\mathrm{r}}(L)$ between 0.1% and 15% relative contact. We call theorists and numericists alike to predict quantities that contain more information than $a_{\mathrm{r}}(L)$ and provide information on how to submit predictions. Examples for quantities of interest are the mean gap or contact stiffness as a function of load as well as distributions of contact patch size, interfacial stress, and interfacial separation at a reference load. Numerically accurate reference results will be disseminated in subsequent work including an evaluation of the submitted results.

I. INTRODUCTION

2016 marks the 50th anniversary of the pioneering approach by Greenwood and Williamson (GW) to describe quantitatively the contact mechanics of nominally flat, but microscopically rough surfaces[1]. The field still thrives, in part due to theoretical advances reducing a highly complex problem to one that can be handled on small-scale computers. The arguably most prominent publications on contact mechanics since the GW paper are the GW-inspired work of Bush, Gibson, and Thomas[2] and the scaling theory proposed by Persson[3]. There has also been much progress in the brute-force solution to contact mechanics. It is now possible to simulate systems that are sufficiently large to mimic the multi-scale nature of surfaces while reaching the continuum limit through sufficiently fine discretization at the small scale[4,5].

Comparisons between theoretical predictions and rigorous simulations — making no uncontrolled approximations beyond the model assumptions — are usually limited to the question if a model reproduces the linearity between load and contact area[4,6–9]. Such comparisons are weak tests because theories merely need to reproduce a single proportionality coefficient while they usually depend on more than one adjustable parameter, which may not even be well defined from experiment or the model definition. The adjustable parameter thereby becomes effectively a fit parameter. An important such term is the scale-dependent radius of curvature of an asperity[10], which plays a critical role in asperity-based models.

Comparisons of theories and rigorous simulations beyond the proportionality coefficient of load and true contact area have been scarce. Notable examples are the analysis of the following quantities: the gap distribution function[11], the dependence of mean gap or contact stiffness on load[12,13], or the interfacial stress spectrum[14,15].

So far, the in-depth comparisons between theory and rigorous simulations have mainly focused on adhesionless contacts, while adhesive interfaces have been even more scarce. The reason for this may be that modeling short-range adhesion in continuum models places large demands on simulations while finite-range adhesion is usually more involved in theoretical approaches. In fact, handling short-range adhesion in simulations of single-asperity contacts and reproducing (closely) the famous analytical results by Johnson, Kendall, and Roberts (JKR)[16] is not easy to achieve. A fine discretization is required close to the contact line[17]. Thus, a rigorous, numerical approach to short-range adhesion in mechanical contacts, irrespective of it being based on a finite-element or boundary-value method remains difficult.

In the following, we describe the model in section II. Selected results are presented in section III while section IV contains a list of quantities to be computed and some discussion of these quantities. The final section V summarizes the rules for the competition.

II. MODEL

A. Surface Topography

We produced our surface realization by drawing random numbers for the Fourier transform of the height profiles $\tilde{h}(\mathbf{q})$ having a mean of zero and, on average, a second moment defined by the height spectrum

$$C(q) \equiv \left\langle |\tilde{h}(\mathbf{q})|^2 \right\rangle \tag{1}$$

$$= C(q_{\mathrm{r}}) \times \begin{cases} 1 & \text{for } \lambda_{\mathrm{r}} < 2\pi/q \leq \mathcal{L} \\ (q/q_{\mathrm{r}})^{-2(1+H)} & \text{for } \lambda_{\mathrm{s}} \leq 2\pi/q < \lambda_{\mathrm{r}} \\ 0 & \text{else.} \end{cases}$$

Here, $\mathcal{L} = 0.1$ mm is the linear dimension in x and y of the periodically repeated simulation cell, $\lambda_r = 20$ μm is the roll-off wavelength, $q_r = 2\pi/\lambda_r$, and $\lambda_s = 0.1$ μm is the short wavelength cutoff, below which no roughness is considered. Finally, H is called the Hurst roughness exponent. A graph showing the spectrum is presented in Fig. 1. The features of the spectrum are similar to those summarized recently by Persson[18].
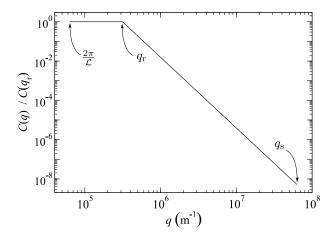

FIG. 1: Height spectrum $C(q)$ from which the height distribution is drawn. It is normalized to its value at the roll-off wavenumber q_r.

One might argue that introducing a cutoff at small wavelength is artificial. However, we see this as necessary in order to make it possible to compare simulations to continuum theories. For similar reasons, we prefer a hard-wall interaction over finite-range repulsion. Even if the latter might be more realistic and, in some ways, easier to handle numerically (e.g., when relaxing the displacement field with a conjugate gradient method), hard-wall repulsion allows us to define unambiguously points of contact and interfacial separation.

The specific surface realization drawn from the spectrum is depicted in Fig. 2. We normalize the height spectra such that the root-mean-square gradient of the height is $\bar{g} = 1$. Furthermore, we shift the heights such that the minimum value is zero. Further characteristics of the surface topography are: mean height $\langle h \rangle = 2.633$ μm, maximum height $h_{max} = 5.642$ μm, and a root-mean square height fluctuation of $\sqrt{\langle \delta h^2 \rangle} = 0.762$ μm with $\langle \delta h^2 \rangle \equiv \langle h^2 \rangle - \langle h \rangle^2$. The inverse root-mean-square curvature, which one may interpret as a typical local radius of curvature, is $R_c = 60$ nm.

The surface is pressed down against an originally flat elastic manifold. Thus, the first points of contact occur at small height, i.e., in the dark areas of Fig. 2. The surfaces can be downloaded from the Internet. Links are provided at http://www.lms.uni-saarland.de/contact-mechanics-challenge/.
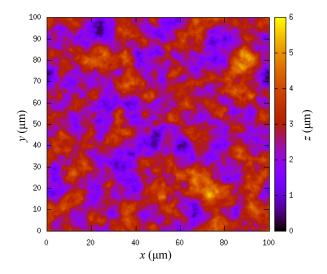

FIG. 2: Height profile of the random surface that was produced from the spectrum shown in Fig. 1.

B. Elasticity, external load, and adhesion

We assume the small-slope approximation, which forms the basis for essentially any contact mechanics theory. All roughness is mapped to the indenter, while all compliance is assigned to the substrate with a contact modulus of $E^* = 25$ MPa, which is characteristic for rubber. Here, $E^* \equiv E/(1 - \nu^2)$, where E is the Young's modulus and ν the Poisson ratio. We leave ν unspecified, as we focus exclusively on normal displacements.

The external default pressure acts homogeneously across the system. It is set to 0.01 $E^*\bar{g}$=250 kPa. In other words, the total load on the simulated area of 0.01 mm² is 2.5 mN. The elastically deformable solid is assumed to be semi-infinite. Mean displacements shall refer to that of the layer pressed against the counterface and not to the layer onto which one would exert external forces experimentally.

Short-range repulsion is realized with a hard-wall interaction, that is, the indenter is not allowed to penetrate the rigid substrate. In addition, the two surfaces interact with a finite-range adhesion according to

$$v[g] = -\gamma_0 \int d^2r \exp\{-g(\mathbf{r})/\rho\}, \qquad (2)$$

where $\gamma_0 = 50$ mJ/m² is the surface energy at perfect contact, $g(\mathbf{r})$ is the local gap or interfacial separation as a function of the in-plane coordinate $\mathbf{r}$, and $\rho = 2.071$ nm. We note that the exponential cohesive zone model used here gives essentially identical results to the analytical solutions of Maugis[19], who used Dugdale's model for adhesion, see Figs. 9 and 10 in Ref. 17.

Defining a local Tabor coefficient according to $\mu_T \equiv R_c^{1/3}(\gamma_0/E^*)^{2/3}/\rho$, we obtain $\mu_T = 3$. This value can certainly be classified as short-range adhesion. This is evidenced in the two bottom panels of Fig. 3. They re-

veal that the adhesive stress is rather localized near the contact lines. See also Figs. 9 and 10 in Ref. 17 from where it is also evident that $\mu_{\mathrm{T}} = 3$ is close to the JKR limit of infinitely short-ranged adhesion, at least as far as contact radius and normal displacement are concerned.

The parameters were chosen to mimic the contact between rubber and a highly polished surface, though the contact modulus may be somewhat at the upper end for practical applications. However, we set up the model such that there is no significant adhesive hysteresis up to moderate contact pressures. Otherwise, functional relations such as $\bar{u}(L)$ or $a_{\mathrm{r}}(L)$ would become history dependent thereby impeding comparisons between theoretical predictions and our simulations.

Pastewka and Robbins[20] found that surfaces only became hysteretic or "sticky" as long as the ratio of "repulsive" contact area and load no longer increases linearly with pressure at small contact area. We found similar results[21] and thus chose an adhesion such that the total contact area is increased by roughly 50% compared to the adhesionless case — at relative contact areas of a few percent.

C. Summary of default parameters

Two important dimensionless quantities of our default problem are the Tabor parameter $\mu_{\mathrm{T}} = 3$ and the surface root-mean square gradient $\bar{g} = 1$. Additional quantities in SI units are: $E^* = 25$ MPa, $\gamma_0 = 50$ mJ/m^2, $\rho = 2.071$ nm, system size $\mathcal{L} = 0.1$ mm, externally applied pressure $p_0 = 250$ kPa.

It might be beneficial to use a problem-adopted unit system, which is what we do in our own simulations. In this unit system one has: $E^*\bar{g}$ as the unit for pressure and $\mathcal{L}$ as the unit for length. One can then use $E^* = 1$, $\mathcal{L} = 1$, $p_0 = 0.01$, $\gamma_0 = 2 \times 10^{-5}$, and $\rho = 2.071 \times 10^{-5}$.

D. Notes on our numerical solution

We solve the contact model using the Green's function molecular dynamics (GFMD) method as described in Ref. 5. The short-ranged adhesion puts large demands on the discretization. Reaching convergence necessitates fine discretization, in particular for adhesive necks forming near contact lines. We found that a discretization of $a = O(\lambda_{\mathrm{s}}/64)$ is sufficient for most purposes and consequently produce reference data on systems with $2^{16} \times 2^{16} \approx 4 \times 10^9$ discretization points on the surface. In some cases, we use $a = O(\lambda_{\mathrm{s}}/128)$ or $\approx 16 \times 10^9$ grid points to ensure that results have sufficiently closely converged to the continuum limit. Using a fine-tuned value for the damping, the system can be typically relaxed within a few thousand time steps, although equilibration at the smallest investigated loads, leading to 0.3% relative contact, necessitates roughly ten times longer simulations.

III. SELECTED RESULTS

A. Configurations at the reference load

We present some selected results, in order to give theorists and modelers the opportunity to ensure that results are in the correct ballpark and/or that units have been implemented correctly. However, it is of no interest to us to receive explanations for why a given theory may be consistent with the provided results. Only true predictions, rather than "post"-dictions, can enter the competition and only predictions will be credited in a future paper assessing the value of the submitted data.

We first show the gap geometry as well as the interfacial stress in a cross section through our system in Fig. 3. We took the geometry as defined above but multiplied the default values for adhesion and load by some factor to make it difficult for participants of the competition to deduce results for the gap. Figure 3 should nevertheless give an impression of the problem's complexity. In particular, it shows the need of a fine discretization near contact lines. In this model, material points at the contact line experience the highest tensile stresses of magnitude γ_0/ρ.
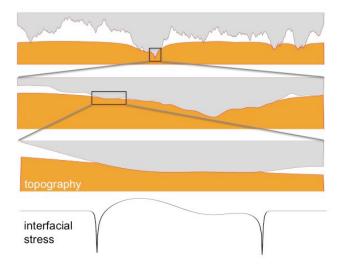

FIG. 3: Contact geometry at different magnifications (three top panels) and local interfacial stress (bottom panel) for the reference geometry. The cut runs through the system shown in Fig. 2 at $x = 50$ μm. Normal and lateral scale differ in all panels. Rectangles highlight the region shown at larger magnification one panel below. Values for adhesion and load differ from their default values by some factor. Only the Tabor coefficient was kept at its reference value of $\mu_{\mathrm{T}} = 3$.

B. Relative contact area as a function of load

The relative contact for moderate loads is shown in Fig. 4. The default load or pressure corresponds to the

value $\tilde{p} \equiv p/E^*\bar{g} = 0.01$. The proportionality coefficient between a_r and $\tilde{p}$ is slightly greater than three, i.e., it is increased by roughly 50% as compared to the adhesionless case.
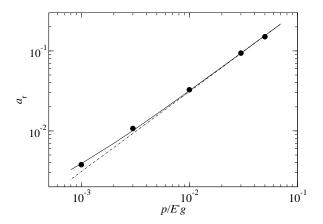

FIG. 4: Relative contact area a_r as a function of the reduced pressure $\tilde{p} = p/E^*\bar{g}$ for the default system. The dashed line shows a linear relation, while the solid line is meant to guide the eye.

IV. QUANTITIES TO BE PREDICTED

In this competition, we focus on physical observables that derive from the interfacial separations field and the stress field. Since we can only run a limited number of simulations for comparison, we need to restrict the number of pertinent observables. We therefore chose one reference point, in which all variables describing the system are fixed and ask competitors to predict various properties that can be defined on that system. We also allow for predictions on how selected observables **vary** with **one single parameter keeping all others fixed** at their values defined in section II C.

1. Distribution of contact patch size.
   Suitable representations for this observable are used in Figs. 4 and 5 of Ref. 22.

2. Contact area as a function of load or pressure.
   Here, we are interested in data for a_r approaching unity, i.e., above 75% contact. Moderate contact areas can too easily deduced by extrapolating results presented in this work. To reveal the asymptotic behavior at large loads, a representation of the $a_r(p)$ relationship as shown in Fig. 1 of Ref. 23 is certainly acceptable.

3. Gap distribution function.
   As an example we refer to Fig. 9 of Ref. 11. Please use logarithmic axes when asymptotic behavior might be unclear otherwise.

4. Interfacial stress distribution function.
   Here, we ask to plot the stress on a linear scale and the probability to find a given stress on a logarithmic scale similar to the way how it is done in Fig. 9 of Ref. 24.

5. Interfacial stress spectrum.
   Again, we can only consider calculations for the default parameters. Examples are given in Figs. 6–8 of Ref. 14.

6. Contact area as a function of the Tabor coefficient.
   All model parameters other than μ_T shall be kept constant. The submitted results should be similar in representation as Fig. 9 in Ref. 17, except, of course, that the contact radius has to be replaced with (relative) contact area and the single-asperity geometry with the given geometry. Please use a logarithmic axis for μ_T. The interesting behavior is found for Tabor parameters less than the default value, i.e., when short-range adhesion crosses over to long-range adhesion. As a clue to the solution, we reveal that the behavior is monotonic but "interesting" around the point where the mean gap has a local extremum.

7. Mean gap or normal displacement (of the layer pressed against the counterface) as a function of the Tabor coefficient.
   Again, all quantities but the Tabor coefficient (or interaction range) should be kept at their default values. Here we refer to Fig. 10 in Ref. 17 and ask again to use a logarithmic representation for the Tabor coefficient.
   A brief discussion might be helpful: As in single-asperity contacts, the mean gap (displacement) initially decreases (increases in magnitude) when μ_T is reduced from its reference value. However, for the investigated contact geometries, this trend must eventually reverse, as for finite or periodically repeated contacts, the adhesive extra load (per unit area) disappears when μ_T approaches zero. Finding the value of μ_T at which the mean gap has its local extremum is a "challenge in the challenge", even if the adhesive interaction range at which this extremum is located, might not be practically relevant.

8. Mean gap or normal displacement as a function of load.
   This quantity has been predicted numerous times by various authors for non-adhesive surfaces, for example, in Fig. 5 of Ref. 11. In that plot it would have been beneficial to use a logarithmic representation for the abscissa, as it would have allowed one to see the asymptotic behavior at small mean separation.
   We do not ask for the interfacial stiffness as a function of load as it follows from the mean gap by

differentiation. Thereby, it does not provide new information.

9. Gap and stress along a cross section.
Participants using numerical methods, e.g., homogenization, are invited to submit results on gap and stress (with units) for the cross section at $x = 50 \, \mu$m shown in Fig. 3. We can smooth the true (microscopic) stress to make a meaningful comparison to homogenization or related approaches.

V. HOW TO SUBMIT

Please summarize your results in a PDF, which you e-mail to: martin.mueser@mx.uni-saarland.de. PDFs should not exceed 5 MB and be sent by May 31, 2016.

The number of figures is limited to ten. Their format should be similar to the ones referred to in the previous section. You are also invited to describe the method with which your data was produced. It will help us to advertise your results and your method if the description is to the point, i.e., complete but brief.

If your simulations are deemed successful (committee: Prof. Martin Müser, Prof. Jim Greenwood, Prof. Wilfred Tysoe, and Prof. Nicholas Spencer), we offer to present your data in a publication in Tribology Letters. If you agree to having your data disseminated and if you agree to our write-up, we will ask for your data (which we receive preferentially as ascii). Once your data has been received and processed, you will be offered co-authorship. If you disagree, we will not use your data.

[1] J. A. Greenwood and J. B. P. Williamson. Contact of nominally flat surfaces. *Proc. R. Soc. London*, A295:300, 1966.

[2] A. W. Bush, R. D. Gibson, and T. R. Thomas. Elastic contact of a rough surface. *Wear*, 35:87, 1975.

[3] B. N. J. Persson. Theory of rubber friction and contact mechanics. *J. Chem. Phys.*, 115:3840–3861, 2001.

[4] S. Hyun, L. Pei, J.-F. Molinari, and M. O. Robbins. Finite-element analysis of contact between elastic self-affine surfaces. *Phys. Rev. E*, 70:026117, 2004.

[5] N. Prodanov, W. B. Dapp, and M. H. Müser. On the contact area and mean gap of rough, elastic contacts: Dimensional analysis, numerical corrections and reference data. *Tribol. Lett.*, 53:433–448, 2014.

[6] C. Campañá and M. H. Müser. Contact mechanics of real vs. randomly rough surfaces: A Green's function molecular dynamics study. *EPL*, 77:38005, 2007.

[7] G. Carbone and F. Bottiglione. Asperity contact theories: Do they predict linearity between contact area and load? *J. Mech. Phys. Solids*, 56:2555–2572, 2008.

[8] M. Ciavarella, G. Demelio, J. R. Barber, and Y. H. Jang. Linear elastic contact of the Weierstrass profile. *Proc. Roy. Soc. A*, 456:387–405, 2000.

[9] M. Paggi and M. Ciavarella. The coefficient of proportionality κ between real contact area and load, with new asperity models. *Wear*, 268:1020–1029, 2010.

[10] J. A. Greenwood and J. J. Wu. Surface roughness: An apology. *Meccanica*, 36:617–630, 2001.

[11] A. Almqvist, C. Campañá, N. Prodanov, and B. N. J. Persson. Interfacial separation between elastic solids with randomly rough surfaces: Comparison between theory and numerical techniques. *J. Mech. Phys. Solids*, 59:2355–2369, 2011.

[12] L. Pastewka, N. Prodanov, B. Lorenz, M. H. Müser, M. O. Robbins, and B. N. J. Persson. Finite-size effects in contacts between self-affine surfaces. *Phys. Rev. E*, 87:062809, 2013.

[13] R. Pohrt, V. L. Popov, and A. E. Filippov. Normal contact stiffness of elastic solids with fractal rough surfaces for one-

and three-dimensional systems. *Phys. Rev. E*, 86:026710, 2012.

[14] C. Campañá, M. O. Robbins, and M. H. Müser. Elastic contact between self-affine surfaces: comparison of numerical stress and contact correlation functions with analytic predictions. *J. Phys.: Condens. Matter*, 20:354013, 2008.

[15] B. N. J. Persson. On the elastic energy and stress correlation in the contact between elastic solids with randomly rough surfaces. *J. Phys. Condens. Matter*, 20:312001, 2008.

[16] K. L. Johnson, K. Kendall, and A. D. Roberts. Surface energy and the contact of elastic solids. *Proc. Roy. Soc. A*, 324(6):301–313, 1971.

[17] M. H. Müser. Single-asperity contact mechanics with positive and negative work of adhesion. *Beilstein J. Nanotechnol.*, 5:419–437, 2014.

[18] B. N. J. Persson. On the fractal dimension of rough surfaces. *Tribol. Lett.*, 54:99–106, 2014.

[19] D. Maugis. Adhesion of spheres: The JKR-DMT transition using a Dugdale model. *J. Colloid Interface Sci.*, 150:243–269, 1992.

[20] L. Pastewka and M. O. Robbins. Contact between rough surfaces and a criterion for macroscopic adhesion. *Proc. Natl. Acad. Sci.*, 111(9):3298–3303, 2014.

[21] M. H. Müser, A dimensionless measure for adhesion and eects of the range of adhesion in contacts of nominally at surfaces, Tribol. Int. (in press).

[22] C. Campañá. Using green's function molecular dynamics to rationalize the success of asperity models when describing the contact between self-affine surfaces. *Phys. Rev. E*, 78:026110, 2008.

[23] W. B. Dapp, N. Prodanov, and M. H. Müser. Systematic analysis of persson's contact mechanics theory of randomly rough elastic surfaces. *J. Phys.: Condens. Matter*, 226:355002, 2014.

[24] G. Carbone, M. Scaraggi, and U. Tartaglino. Adhesive contact of rough surfaces: Comparison between numerical calculations and analytical theories. *Eur. Phys. J. E*, 30:65–74, 2009.